

Fractalization of Rectangular Rings

or

Chainese Spoken Here

1. Introduction

An interesting aspect of statistical geometry fractals is the random chain-linkage of "donut" shapes with holes, i.e., *random topology*. This was first seen in fractalizations of toroidal rings constructed by Paul Bourke. This phenomenon only occurs for more than two Euclidean dimensions.

Basic ideas of statistical geometry fractals [1] tell us that it is possible to fill space completely "in the limit" with rings, some of them (randomly) linked in chains. The present study was undertaken to get a better understanding of this bizarre-sounding idea: "You can fill all space with rings." The answer to this question is "Yes." If the question is "Can you fill all space with rings every one of which has at least one link?", the answer appears to be "No." If the question is "Can you create a rectangular-ring fractal with better than 95% of the rings chain-linked in a single chain?", the answer is "Yes."

The first part of this report (secs. 2-4) describes the geometry of the rings and the computation scheme. Section 5 describes the statistics of fractalization, and poses the question "What is the probability of finding a chain containing k links?". The work was a joint effort by Bourke and Shier, with the latter doing most of the computation and code development, and the former checking code validity with three-dimensional ray-traced images, and making drawings of the finished product.

2. Description

While toroidal rings make fascinating images, they have some limitations for systematic studies of chain-linking. One would like to compute whether a given pair of rings is chain-linked or not. This is easier if one uses right-angled shapes as shown in Fig. 1.

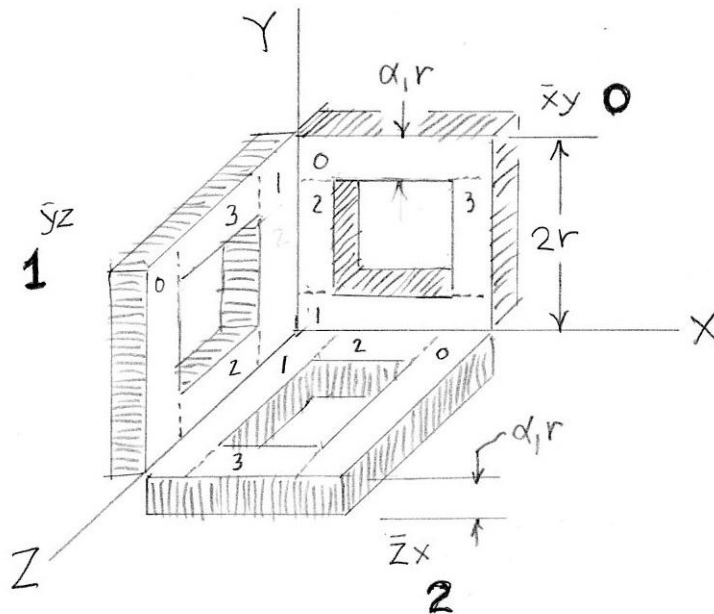


Fig. 1. Geometric specification of the three rings (not to scale). The bold numbers show the *nsymb* numbers for each orientation. The small numbers on each "brick" show how the bricks are arranged in the ring. This sketch

shows the orientation and dimensions of the rings and bricks, but the origin of coordinates used in the data base lies at the centers of the rings (Fig. 2).

The ring can be thought of as a thin flat square slab having outer edge lengths $2r$ on the long sides and thickness $\alpha_1 r$, with a square hole cut in the middle. A right-angled cut through any arm of the ring is a square which has dimensions $\alpha_1 r$ by $\alpha_1 r$. It is required that $0 < \alpha_1 < 1$. The bounding region for fractalization is a cube.

It can be seen from Fig. 1 that each ring is made up from 4 "bricks"¹. Overlap is tested by testing all 4 bricks of ring A against all 4 bricks of ring B (16 tests). Overlap tests of bricks are quite fast. This overlap test is exact in the sense that its accuracy is limited only by the resolution of the floating point numbers used.

During trials a ring is specified by

- The values of the coordinate points x, y, z at the center of the ring.
- The size r which is half the outer edge length.
- An integer parameter $nsymb$ which is 0 for a ring in the xy plane, 1 for a ring in the yz plane and 2 for a ring in the zx plane (Fig. 1).

With the rings lying in orthogonal planes the number of chain links will be higher than if they have random orientations.

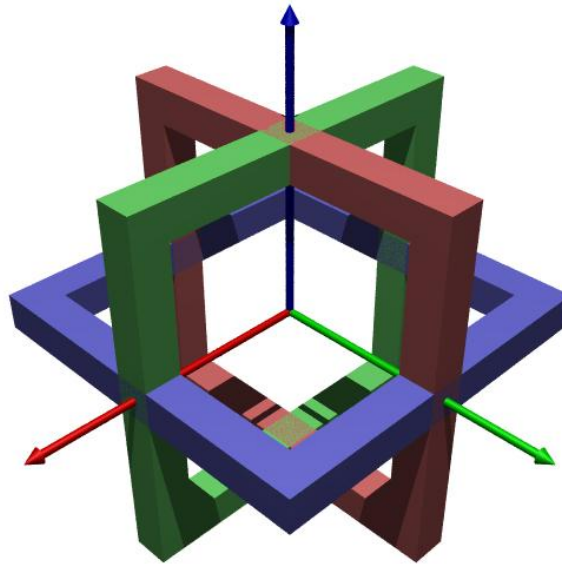


Fig. 2. Local coordinate system for the data base and the computations, showing the three orthogonal ring orientations. The origin of coordinates is at the center of the ring. The x position of a ring is the distance from the origin of coordinates of the bounding cube at one of its corners to the center of the ring. The rings are drawn for $\alpha_1 = 0.2$.

This work uses *periodic boundaries*². An associated question is the treatment of the "redundant"³ rings. Each of the redundant rings is viewed as a separate ring. Because of redundancy if we set out

¹ For present purposes a "brick" is defined as a solid all of whose boundaries are xy , yz , or zx planes. The arrangement of the bricks is somewhat arbitrary and is not required for a geometric specification of the ring, so it is omitted from the data base.

² With inclusive boundaries the rings in (say) the xy plane tend to pile up near the xy sides of the bounding box. With periodic boundaries the sides of the box have much less influence, i.e., the distribution of rings is more random.

to place k nonredundant rings, the total ring count will be somewhat larger than k because we must include the redundant rings.

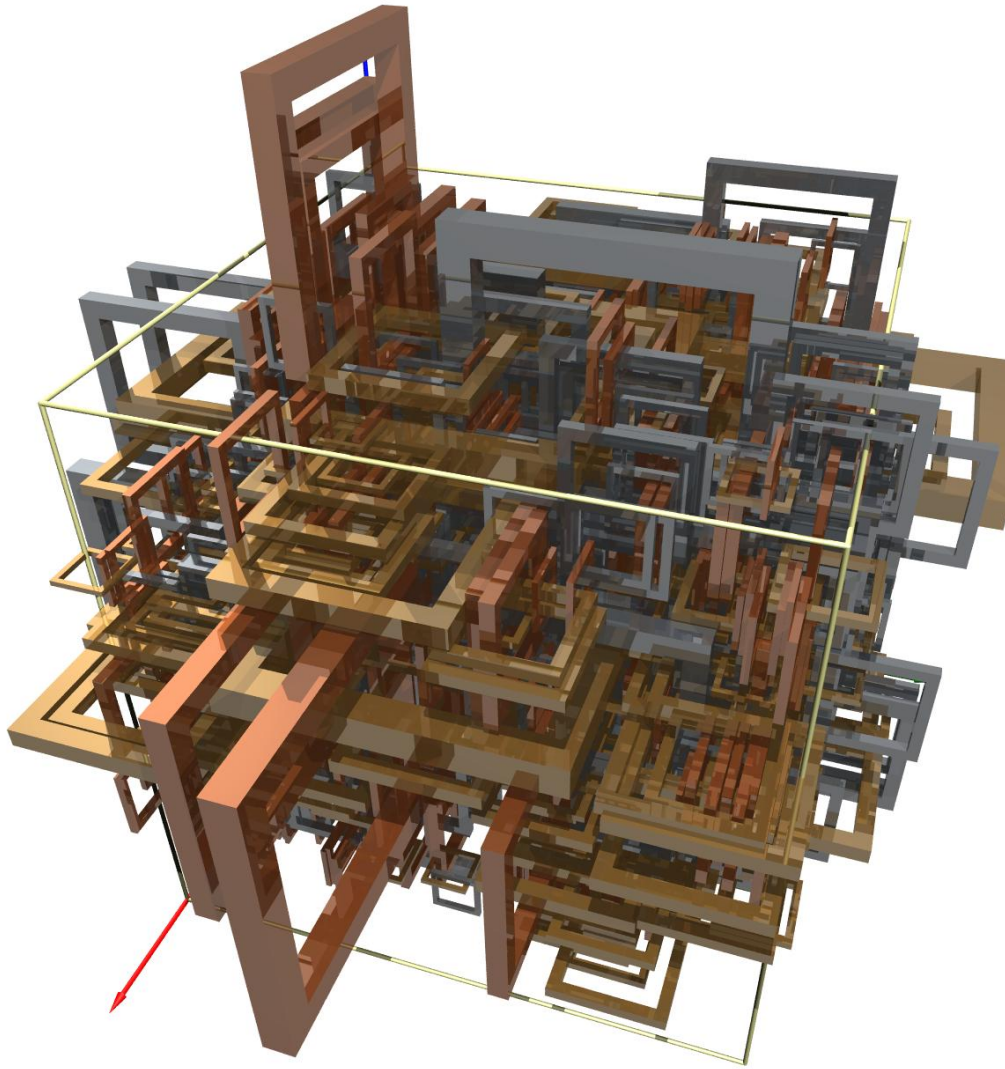


Fig. 3. An example of a large chain extracted from a set of rings fractalized within a cube using periodic boundaries. The round rods show the bounding cube. Every ring is chain-linked to at least one other ring, and many of them have multiple links. A ray-tracing technique has been used to improve visualization of the data. Rings in the xy , yz , and zx planes have different colors. This structure is a 3D "tile" and will join smoothly when repeated with a spacing which is a multiple of the bounding cube edge length, i.e., it has translation symmetry. Close study will show that the rings are "clustered" -- an xy -plane ring is more likely to be close to another xy -plane ring, etc.

³ With periodic boundaries, if a ring crosses the boundary it gets 1, 3, or 7 additional "redundant" rings which have the same size and orientation of the "original" one but are displaced by bounding cube edge lengths. The total volume of the parts of the original and redundant rings which lie within the bounding cube adds up to the volume of a single ring.

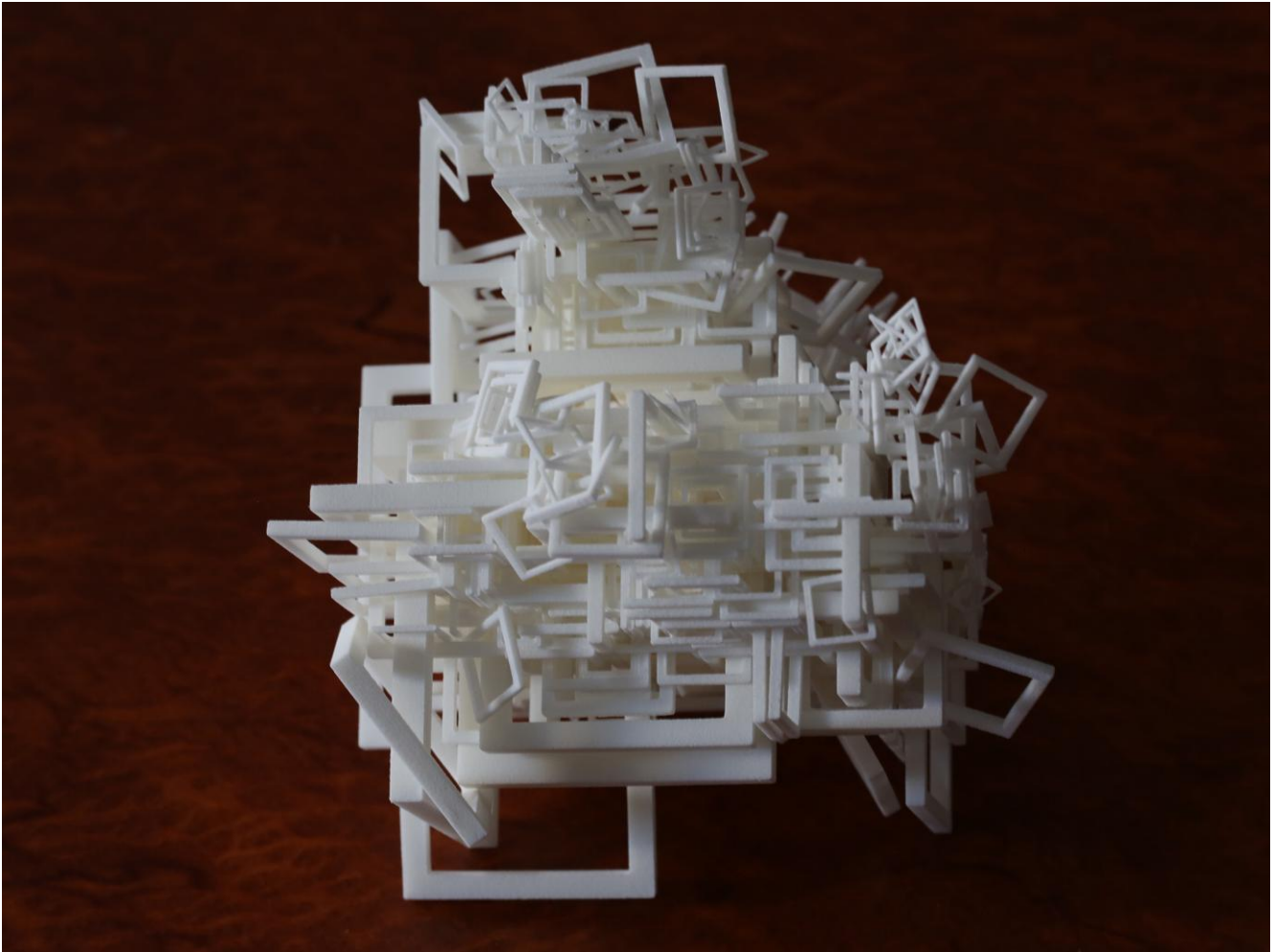


Fig. 4. A physical model of a chain of rings. A description file was prepared by Bourke and sent to a 3D printer with this result. The smaller and less-entangled rings flop around, constrained only by their ring topology.

3. Fractalization

In order to produce a substantial amount of chain linking it is desirable to have α_1 small. If it is too close⁴ to 1.0 chain linking cannot occur ("fat" rings can't be threaded through each other). There is a trade-off between thin rings (much linking) and slow computation (many trials per placement). In general 3D fractalizations are slower than 2D and 1D, and have lower maximum c values.

After early work with inclusive boundaries it was decided to use periodic boundaries. With inclusive boundaries the rings in the xy plane "pile up" near the xy surfaces of the bounding cube, etc.

The *nsymb* parameter is varied cyclically 0, 1, 2, 0, 1, 2, ... at each placement so that there are equal numbers of the 3 orientations.

The *redund* parameter is used to label redundant shapes when periodic boundaries are used. With periodic boundaries the first shape of those that have the same size has *redund* = 1 while all of the others (i.e., those displaced by a bounding cell period) have *redund* = 0.

Also in the data file is an integer *trials* which is the number of trials needed to place the k -th shape. This can be used for statistical studies, and provides a record of how the process proceeded.

4. Chain Links and Data Files

⁴ Chain linking cannot occur if $\alpha_1 > 2/3$ but the algorithm still runs.

With the rectangular shapes used it is fairly straightforward to compute whether two rings are chain-linked. Several observations allow one to speed up this process:

- Rings lying in the same plane cannot chain-link
- Rings distant by more than $(r_A + r_B)$ in x , y , or z cannot chain-link
- If ring A links to ring B, then necessarily ring B links to ring A (offered without proof)
- A ring does not link to itself
- If the "arm width" ($\alpha_1 r$) of A is larger than the hole size ($2r(1-\alpha_1)$) of B they cannot chain-link

The data file first line gives the X, Y, and Z dimensions of the bounding cube (i.e., $0 < x < X$, etc.), the number of rings, and α_1 . This is followed by repeated lines with the following data items (separated by spaces) in the following order:

$x, y, z, r, nsymb, linkct, redund, trials$

All except *linkct* are determined during execution of the algorithm, while *linkct* is found by post-processing of the results.

As α_1 decreases the pattern becomes more sparse, a larger fraction of the rings have linkages, the largest usable c value becomes smaller, and a larger N value is needed to keep the first ring from exceeding the available space.

For each run a file of linkages is created, i.e., an entry "27 304" indicates that ring 27 and ring 304 are mutually chain-linked. The linkage file is further processed to create a table of chains -- all of the ring numbers which belong to a given chain. If there are a total of k rings, the number of linkages can greatly exceed k , and can be as large as $k(k-1)/2$. If there are more linkages than rings it means that on average each ring is linked to several other rings. Many examples of this can be seen in Fig. 3.

From the viewpoint of graph theory the rings can be thought of as vertices and the chain linkages as edges. A more detailed exploration of these graphs may be interesting but is left for future work.

5. Statistics

The statistical question studied is: "What is the probability that a chain of k rings is formed?" There will be unlinked rings, pairwise-linked rings (chain length 1), etc. The largest possible chain would include all of the rings and thus would have more than the number of nonredundant rings as members, i.e., a fractalization done for 100 nonredundant rings might have 113 rings altogether when the redundant rings are included. By linked we mean linked in the topological sense, that it is not possible to separate the two rings without breaking one of them. Linkage is a pairwise property.

The runs were set up with the parameters given in Table 1.

Table 1. Fractalization parameters used in the work.

case	c	N	α_1	rings	runs	linkages	fill, %	avg. trials/placement
1	1.125	14.5	.28	2000	40	~900	46	~9.2k
2	1.114	16	.25	2000	40	~1500	42	~10.2k
3	1.095	19	.21	2000	40	~2400	36	~6.3k
4	1.085	23	.18	2000	40	~3400	32	~6.8k
5	1.075	29	.15	2000	40	~5400	27	~7.4k
6	1.063	35	.125	2000	40	~7800	22	~5.2k

The N and c values were chosen to make the outer edge length (long edge) of the first (largest) ring be approximately 5 units (with a bounding cube edge length of 10 units) and an average trials per placement of 5000-10000. With $\alpha_1 = .28$ the rings are relatively thick and the number of linkages is

much less than the number of rings. With $\alpha_1 = .125$ the rings are quite thin and the number of linkages is substantially larger than the number of rings.

In all of the histograms the leftmost dot gives the number of rings with 3 or 4 members, the next one rings with 5, 6, 7, or 8 members, etc., i.e., the data is grouped logarithmically with each group having a 2x wider range than the last one. The vertical value (y axis) is the total number of times chains within the ring member count range (x axis) were observed in 40 runs.

Column 7 gives the typical total number of linkages between rings. Column 8 gives the percentage fill. Column 9 gives the average trials per placement, from which it can be seen that these were tight-packed runs requiring long searches for placement.

Each dot in a histogram corresponds to the ring member count ranges shown in Table 2.

Table 2. Ring-count boundaries for the histograms. Dot number 1 is the leftmost dot in the histograms.

dot no	1	2	3	4	5	6	7	8	9	10	11
range	3-4	5-8	9-16	17-32	33-64	65-128	129-256	257-512	513-1024	1025-2048	>2048

The x coordinate of a dot in the histograms is taken as the log of the geometric mean of its two boundaries, i.e., the range 5-8 would be plotted as the log of $\sqrt{4 \cdot 8} = 4\sqrt{2}$.

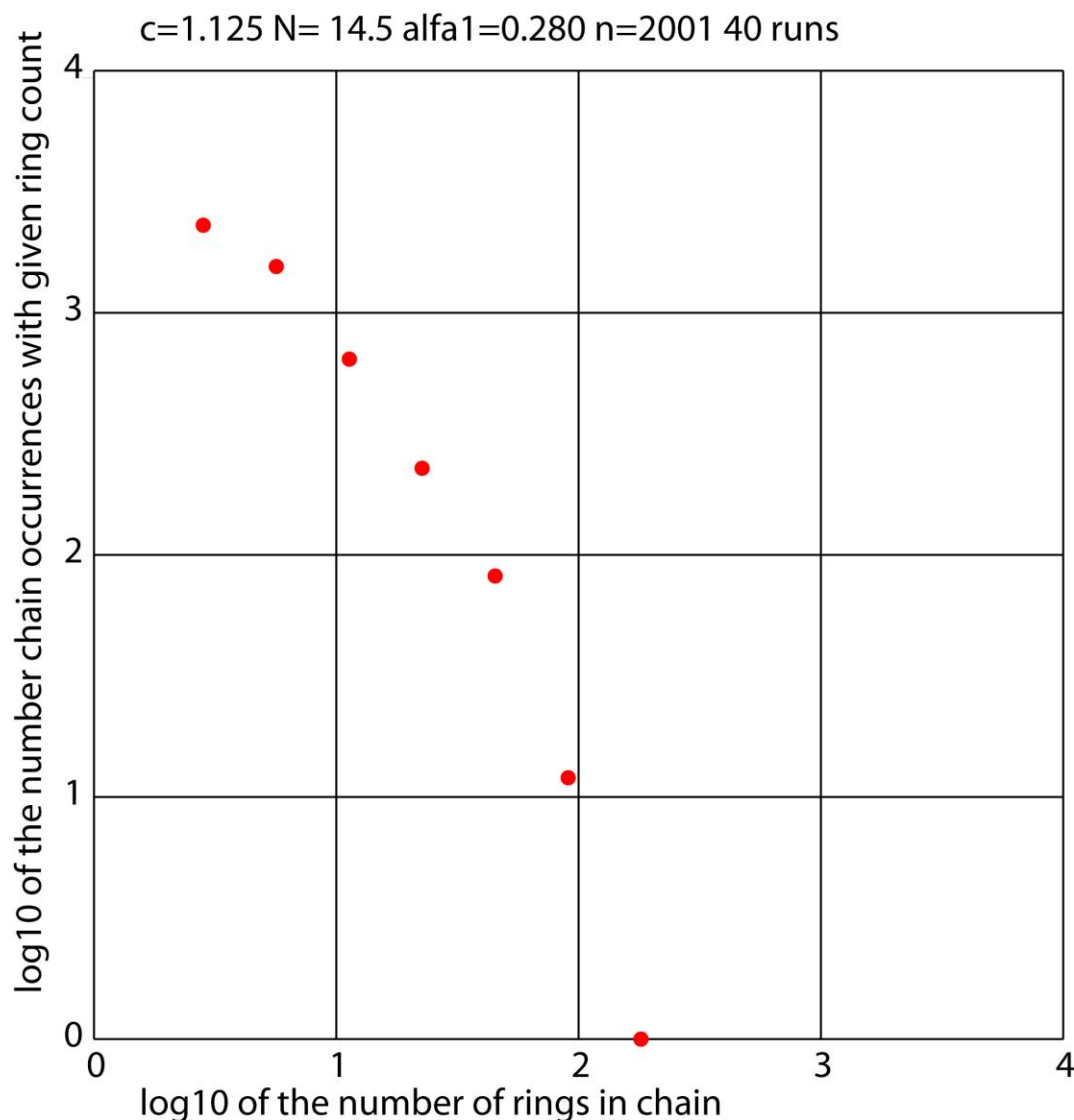


Fig. 5. Log-log histogram for $\alpha_1 = .28$ ("thick" rings). There are no chains with >128 members, and the number of chains falls very rapidly for large member counts. This distribution can be approximated by the lognormal distribution.

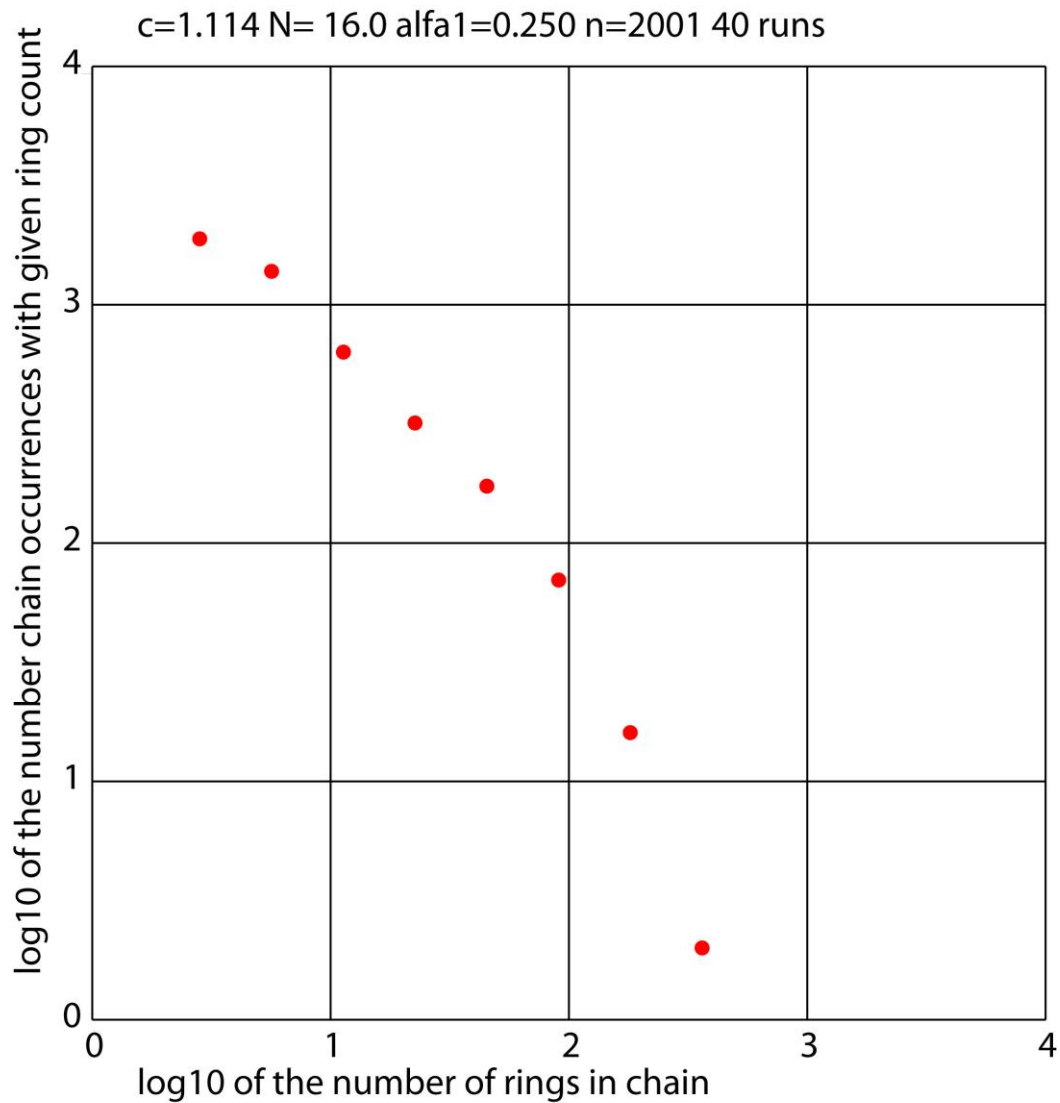


Fig. 6. Log-log histogram for $\alpha_1 = .25$. The rings are thinner and the number of chains with 3-4 members is down slightly, while there are now a few chains with 257-512 members.

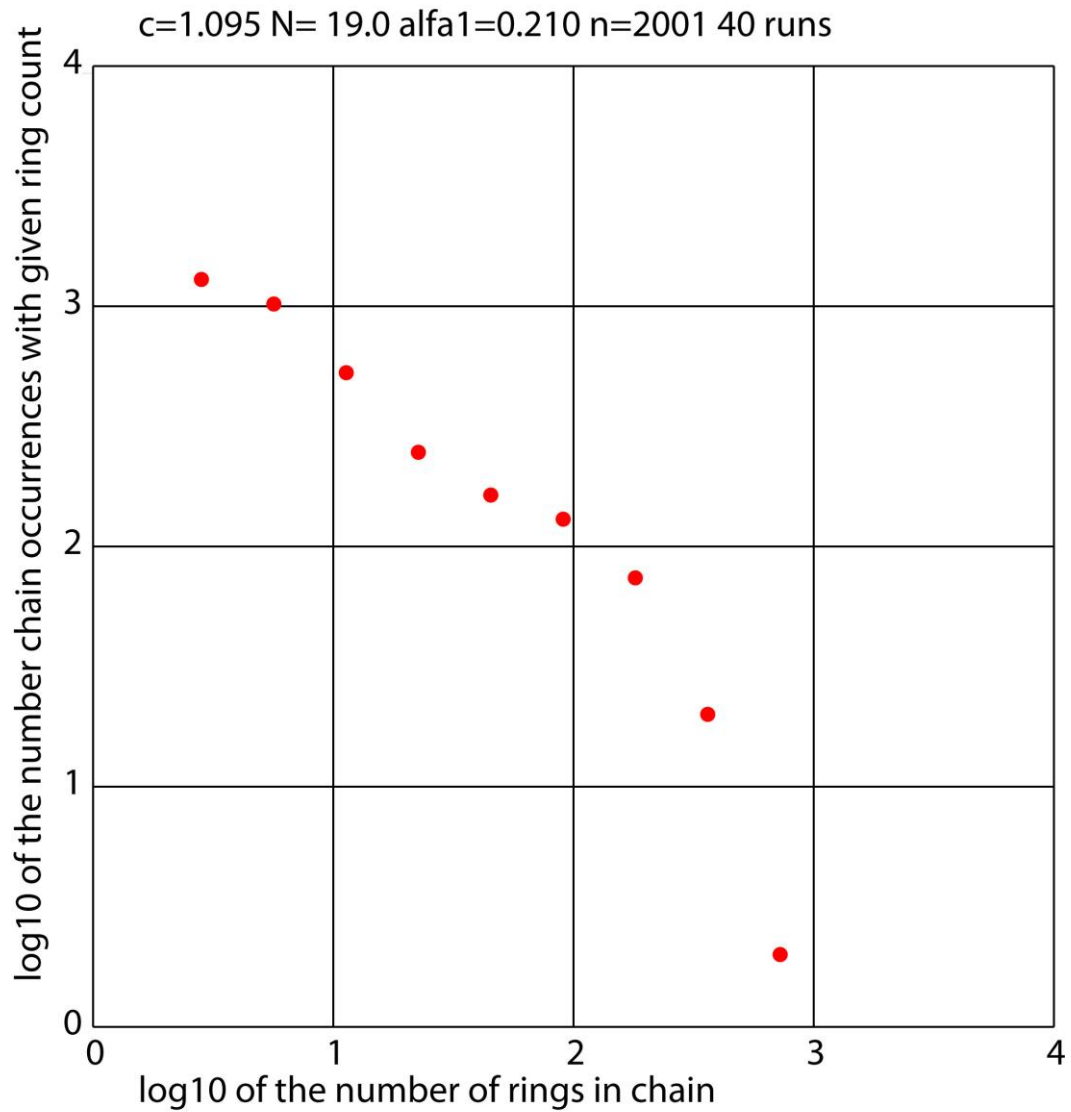


Fig. 7. Log-log histogram for $\alpha_1 = .21$. The rings are thinner than Fig. 6 and the number of chains with 3-4 members is again down substantially, while there are now a few chains with 513-1024 members. The decline in the number of instances versus chain size is less steep than in Fig. 6 and resembles a fat-tailed power law (with approximate exponent -.5) for the first 7 points.

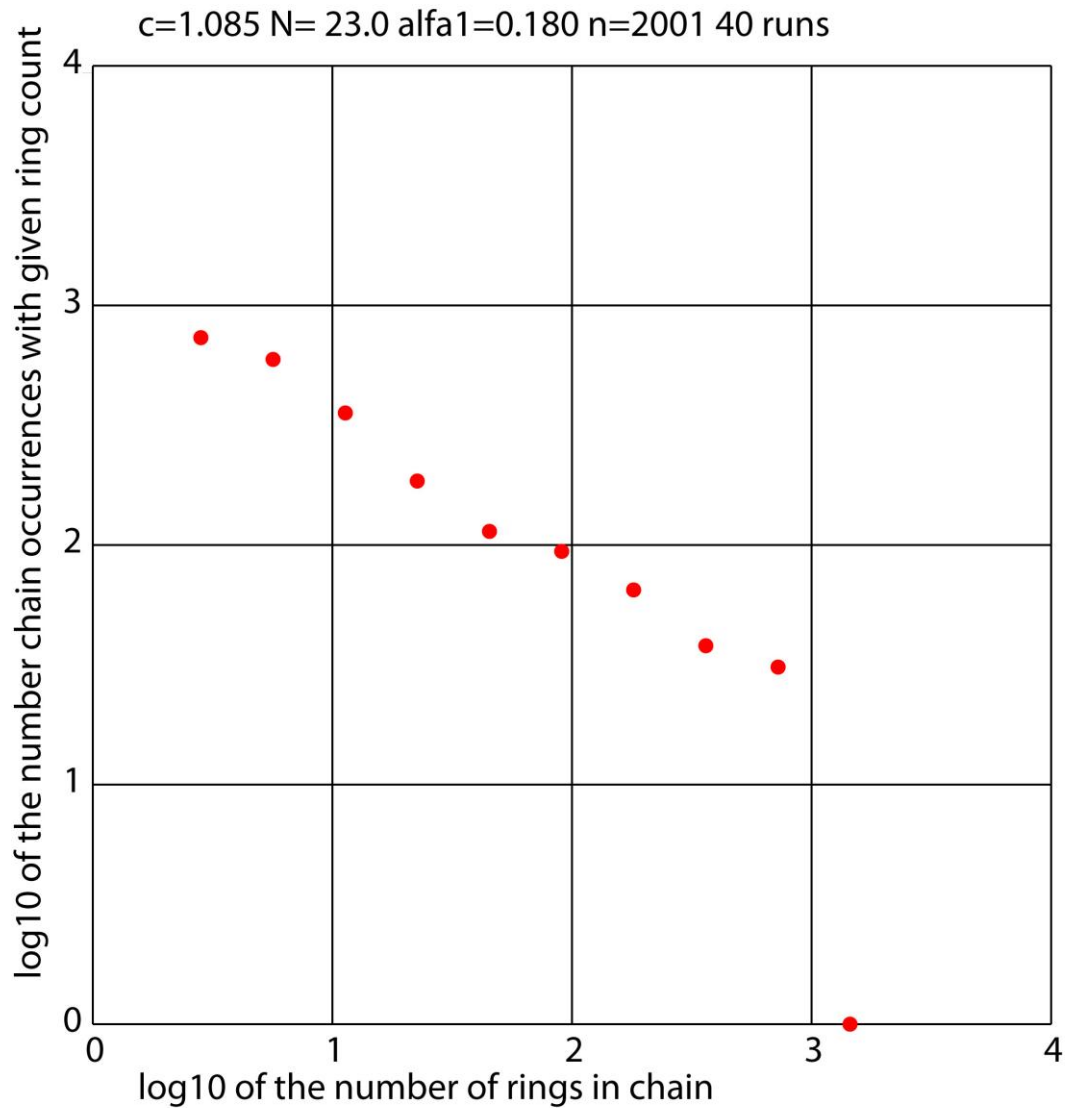


Fig. 8. Log-log histogram for $\alpha_1 = .18$. The rings are thinner than Fig. 7 and the number of chains with 3-4 members is down again, while there is now one chain with 1025-2048 members. The decline in the number of instances versus chain size resembles a fat-tailed power law (with approximate exponent -.5) for the first 9 points.

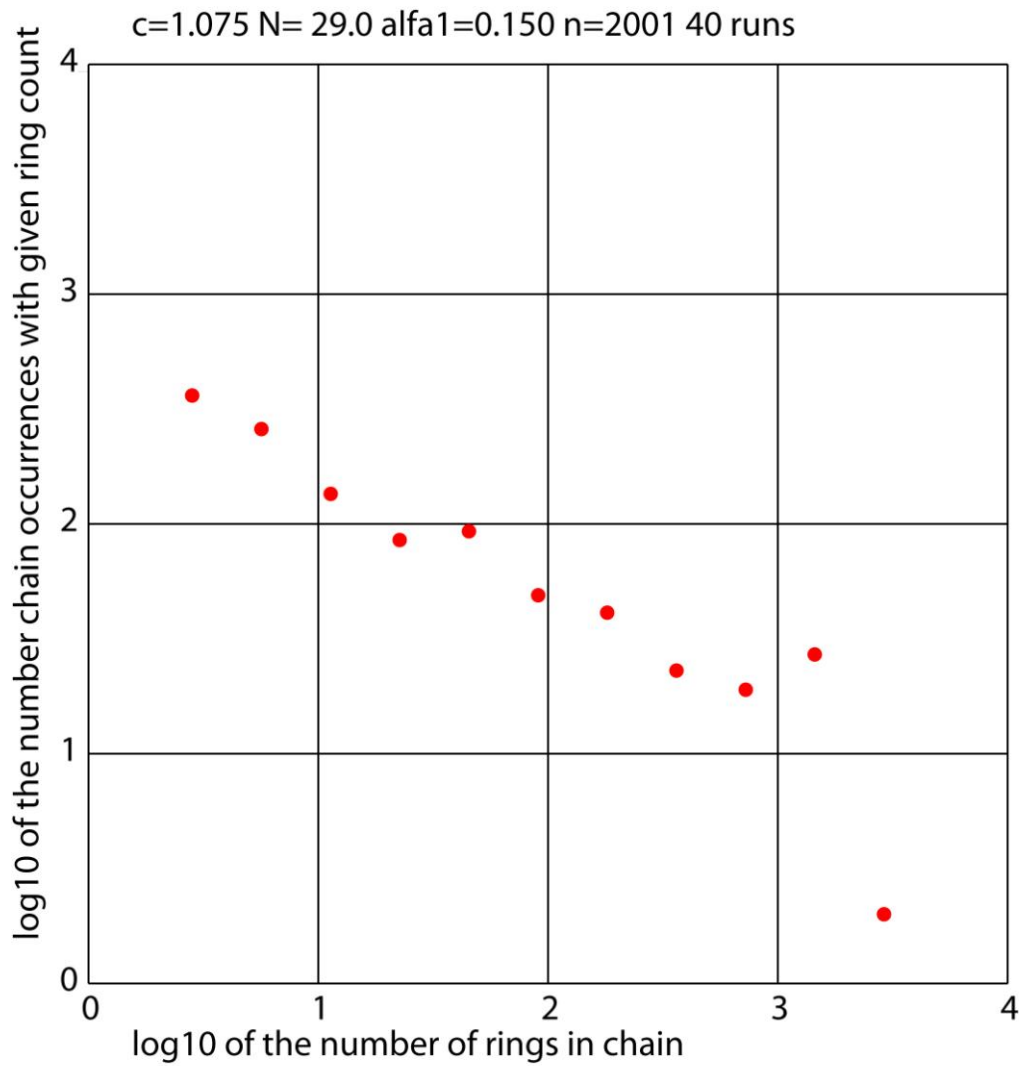


Fig. 9. Log-log histogram for $\alpha_1 = .15$. The rings are thinner than Fig. 8 and the number of chains with 3-4 members is down sharply. The first 9 points follow an approximate power law, but then we have an increase in the number of chains with 1025-2048 members. The largest chains now may include more than half of all the rings. There are two chains with >2048 members, which is possible because of redundant rings.

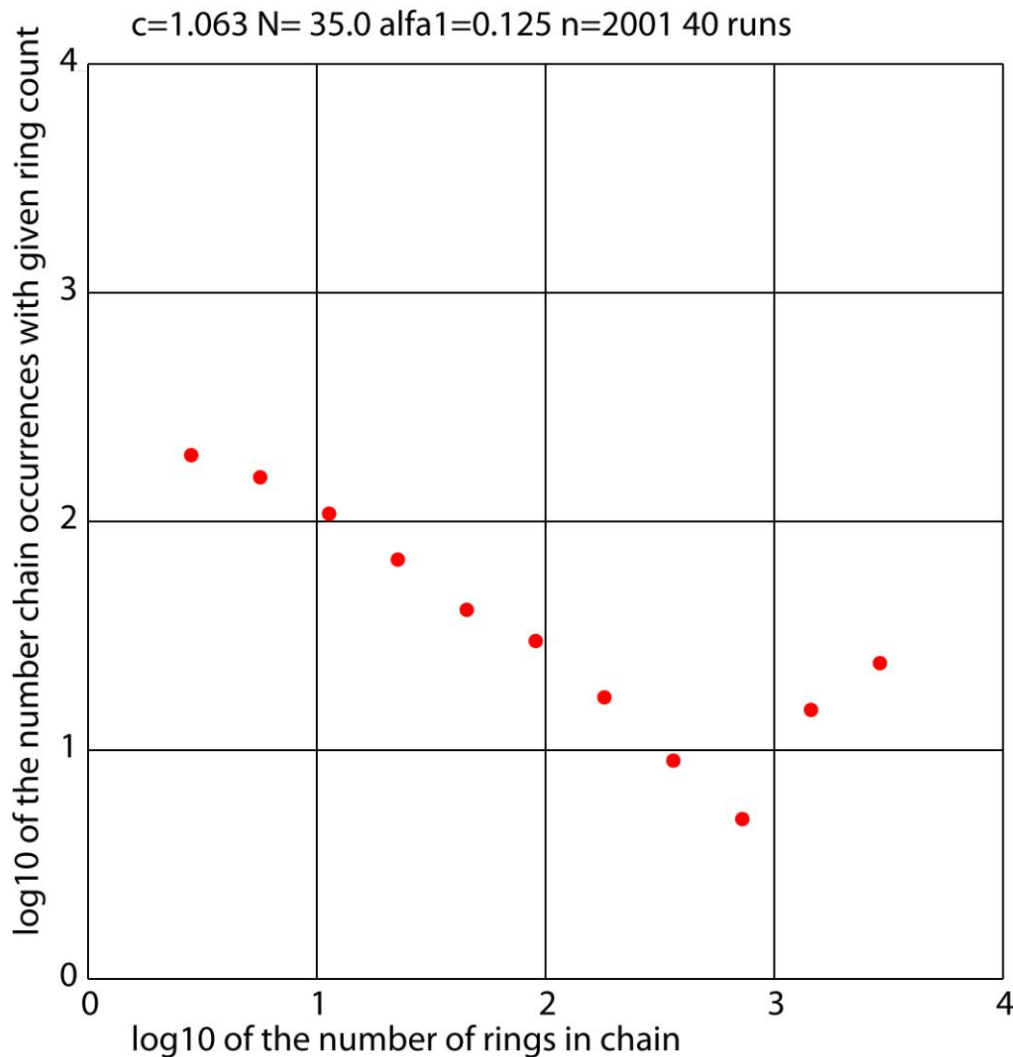


Fig. 10. Log-log histogram for $\alpha_1 = .125$. The rings are thinner than Fig. 9 and the number of chains with 3-4 members is again down sharply. The first few points follow an approximate power law; then there is a dip followed by a sharp increase in the number of chains with >1024 members. The largest chain now includes most of the rings, i.e., a single chain becomes dominant. The runs making up this data had typically around 8000 linkages, so that the average ring was linked to 4 others.

When $\alpha_1 = .28$ the distribution looks like a downward-opening parabola in a log-log plot. The Gaussian distribution has this form in a semilog plot, but not in a log-log plot. Distributions of this kind are called *lognormal*⁵ distributions.

With $\alpha_1 = .125, .15, .18$, and $.21$ a portion of the data gives an approximate straight line corresponding to a negative-exponent power law, but for the largest chains the behavior is quite different. For $\alpha_1 = .125$ and $.15$ there is a minimum in the histogram, with most of the rings in a small number of chains or a single chain.

For the lowest α_1 value (.125) with quite thin rings there is a sort of "chain reaction" (if you pardon the expression) which results in a *single dominant chain*. Just as uranium atoms react producing 2-3

⁵ The lognormal distribution is described in both Wikipedia and Wolfram MathWorld. The lognormal distribution has uses in economics, and the size distributions of some biological objects obey the lognormal distribution. In the latter case one could conclude that the underlying growth processes have a lognormal trend. The lognormal distribution has a probability $p(0) = 0$, which agrees with the fact that there are no chains with zero length.

new neutrons from a single neutron-induced fission, here we get about 4 links for each ring. A closer look at the data shows that the non-dominant chains are few in number and have only small numbers of rings. As the process continues they will become linked to the dominant chain, while a few small new chains are produced. It is improbable that one can achieve 100% linking by this means.

There are several "regimes" of the process for different links/rings ratios. If links \ll rings (large α_1) the chain sizes have a lognormal distribution. If links \gg rings (small α_1) there is a dominant chain which contains most of the rings. In the intermediate case where links \approx rings an approximate power-law trend can be seen.

Linking adds a unique feature to the system, not seen in other 3D fractals to date. The growth of the chains involves a "rich get richer" principle of positive feedback. A chain which has more rings than the others is more likely to link to still more rings. If there are several large chains one can get an even larger chain if there is a lucky linkage which links two large chains by "merger". When links \gg rings (thin rings) the linkage can be relatively "long-range" -- two rings can become linked which are not immediate neighbors.

This system has a large "space" of parameters (c , N , α_1 , etc.). The results described here are just one example. Broader study of this subject is left for future work.

The algorithm was also set up with an additional constraint, that each new ring must not only not overlap any earlier ring, but must have at least one link to an earlier ring. Tests of this were a failure with the parameters used. No run was able to place even 100 rings without stopping. The records of the number of trials needed showed that its increase was much faster than without the all-linked constraint.

6. Reference

The best reference for the algorithm is the Shier-Bourke paper. Copies of the last version to go to the editor can be downloaded at the Shier or Bourke web sites. The formal citation is:

/1/ "An Algorithm for Random Fractal Filling of Space", John Shier and Paul Bourke, Computer Graphics Forum, Vol. 32, Issue 8, pp. 89-97, December 2013.

There is much additional information at the Shier and Bourke web sites.